MDPI

Article

New Alkylpyridinium Anthraquinone, Isocoumarin, C-Glucosyl Resorcinol Derivative and Prenylated Pyranoxanthones from the Culture of a Marine Sponge-Associated Fungus, *Aspergillus stellatus* KUFA 2017

Fátima P. Machado [1,2], Inês C. Rodrigues [1], Luís Gales [1,3], José A. Pereira [1,2], Paulo M. Costa [1,2], Tida Dethoup [4], Sharad Mistry [5], Artur M. S. Silva [6], Vitor Vasconcelos [2,7] and Anake Kijjoa [1,2,*]

[1] ICBAS-Instituto de Ciências Biomédicas Abel Salazar, Rua de Jorge Viterbo Ferreira, 228, 4050-313 Porto, Portugal
[2] Interdisciplinary Centre of Marine and Environmental Research (CIIMAR), Terminal de Cruzeiros do Porto de Leixões, Av. General Norton de Matos s/n, 4450-208 Matosinhos, Portugal
[3] Instituto de Biologia Molecular e Celular (i3S-IBMC), Universidade do Porto, Rua de Jorge Viterbo Ferreira, 228, 4050-313 Porto, Portugal
[4] Department of Plant Pathology, Faculty of Agriculture, Kasetsart University, Bangkok 10240, Thailand
[5] Department of Chemistry, University of Leicester, University Road, Leicester LE 7 RH, UK
[6] Departamento de Química & QOPNA, Universidade de Aveiro, 3810-193 Aveiro, Portugal
[7] FCUP-Faculty of Sciences, University of Porto, Rua do Campo Alegre, s/n, 4169-007 Porto, Portugal
* Correspondence: ankijjoa@icbas.up.pt; Tel.: +351-962712474; Fax: +351-22-206-2232

Abstract: An unreported isocoumarin, (3S,4R)-4-hydroxy-6-methoxymellein (**2**), an undescribed propylpyridinium anthraquinone (**4**), and an unreported C-glucosyl resorcinol derivative, acetyl carnemycin E (**5c**), were isolated, together with eight previously reported metabolites including *p*-hydroxybenzaldehyde (**1**), 1,3-dimethoxy-8-hydroxy-6-methylanthraquinone (**3a**), 1,3-dimethoxy-2,8-dihydroxy-6-methylanthraquinone (**3b**), emodin (**3c**), 5[(3E,5E)-nona-3,5-dien-1-yl]benzene (**5a**), carnemycin E (**5b**), tajixanthone hydrate (**6a**) and 15-acetyl tajixanthone hydrate (**6b**), from the ethyl acetate extract of the culture of a marine sponge-derived fungus, *Aspergillus stellatus* KUFA 2017. The structures of the undescribed compounds were elucidated by 1D and 2D NMR and high resolution mass spectral analyses. In the case of **2**, the absolute configurations of the stereogenic carbons were determined by comparison of their calculated and experimental electronic circular dichroism (ECD) spectra. The absolute configurations of the stereogenic carbons in **6a** and **6b** were also determined, for the first time, by X-ray crystallographic analysis. Compounds **2**, **3a**, **3b**, **4**, **5a**, **5b**, **5c**, **6a**, and **6b** were assayed for antibacterial activity against four reference strains, viz. two Gram-positive (*Staphylococcus aureus* ATCC 29213, *Enterococcus faecalis* ATCC 29212) and two Gram-negative (*Escherichia coli* ATCC 25922, *Pseudomonas aeruginosa* ATCC 27853), as well as three multidrug-resistant strains. However, only **5a** exhibited significant antibacterial activity against both reference and multidrug-resistant strains. Compound **5a** also showed antibiofilm activity against both reference strains of Gram-positive bacteria.

Keywords: *Aspergillus stellatus*; Trichocomaceae; marine sponge-associated fungus; anthraquinones; isocoumarin; C-glucosyl resorcinols; antibacterial activity; antibiofilm activity

1. Introduction

The genus *Aspergillus* (family Aspergillaceae) is one of the most extensively studied genera of filamentous fungi, mainly due to the medical relevance, food spoilage, and industrial application of some of its species. Aspergilli can grow in a wide range of niches, mainly in soils and on dead matter, but some are also capable of colonizing living animal or plant hosts. However, the increasing numbers of *Aspergillus* species have been found in

different niches in the marine environment, from tropical waters [1] to the Arctic [2], and from shallow waters [3] to the deep-sea [4]. In total, approximately 350 *Aspergillus* species have been identified [5].

In the last two decades, marine-derived *Aspergillus* species have attracted tremendous attention from researchers working on marine natural products since they were responsible for a production of the highest numbers of marine fungal metabolites as demonstrated by two review articles, one covering the period of January 1992 to December 2014, reporting 512 metabolites, and another covering the period of 2015 to December 2020, which reported 361 compounds, isolated from marine-derived *Aspergillus* species [6]. It is also worth mentioning that the specialized metabolites produced by marine-derived *Aspergillus* species possess not only structural diversity such as indole alkaloids, diketopiperazine derivatives, meroterpenoids, anthraquinones, isocoumarins, xanthones, *p*-terphenyl derivatives, and peptides, but also a myriad of biological activities [6].

In our pursuit of antibiotic and antibiofilm compounds from marine-derived fungi from tropical seas, we focused our attention on the marine sponge-associated *Aspergillus stellatus* since this fungus has not been extensively investigated. A literature search revealed that a mycotoxin, asteltoxin, was isolated from toxic maize meal cultures of *A. stellatus* Curzi (MRC 277) [7]. In another work, Kamal et al. reported the isolation of tajixanthone, shamixanthone, ajamxanthone, shahenxanthone, najamxanthone, radixanthone, and mannitol from the mycelium of *A. stellatus* Curzi [8]. For this reason, we investigated secondary metabolites from the culture of *A. stellatus* KUFA 2017, isolated from a marine sponge, *Mycale* sp., which was collected from the coral reef at the Samaesan Island, in the Gulf of Thailand.

Fractionation of the ethyl acetate (EtOAc) extract of the culture *A. stellatus* KUFA 2017 by column chromatography of silica gel, followed by purification by preparative TLC, Sephadex LH-20 column and crystallization, led to the isolation of undescribed (*3S,4R*)-4-hydroxy-6-methoxymellein (**2**), stellatanthraquinone (**4**), and acetyl carnemycin E (**5c**), as well as the previously reported *p*-hydroxybenzaldehyde (**1**) [9], 1,3-dimethoxy-8-hydroxy-6-methylanthraquinone (**3a**) [10], 1,3-dimethoxy-2,8-dihydroxy-6-methylanthraquinone (**3b**) [11], emodin (**3c**) [12] and 5[(3*E*,5*E*)-nona-3,5-dien-1-yl]benzene (**5a**) [13], carnemycin E (**5b**) [13], tajixanthone hydrate (**6a**) [14,15], and 15-acetyl tajixanthone hydrate (**6b**) [16]. (Figure 1). The structures of the undescribed compounds were established on the basis of an extensive analysis of their 1D and 2D NMR as well as HRMS spectra. In the case of **2**, the absolute configurations of their stereogenic carbons were established by comparison of their experimental and calculated electronic circular dichroism (ECD) spectra. Additionally, the absolute structures of tajixanthone hydrate (**6a**), and 15-acetyl tajixanthone hydrate (**6b**) were also unambiguously determined by X-ray analysis for the first time.
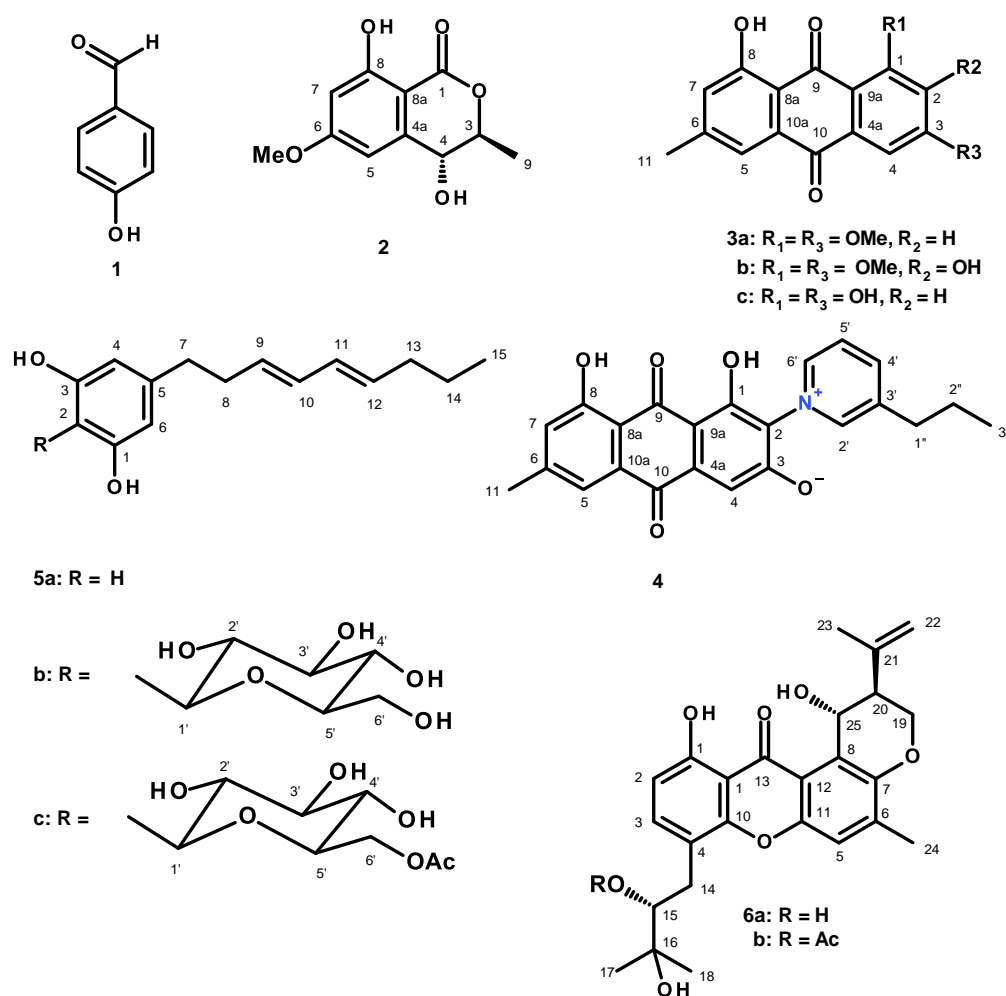
Figure 1. Structures of *p*-hydroxybenzaldehyde (**1**), (3*S*,4*R*)-4-hydroxy-6-methoxymellein (**2**), 1,3-dimethoxy-8-hydroxy-6-methylanthraquinone (**3a**), 1,3-dimethoxy-2,8-dihydroxy-6-methylanthraquinone (**3b**), emodin (**3c**), stellatanthraquinone (**4**), 5[(3*E*,5*E*)-nona-3,5-dien-1-yl]benzene-1,3-diol (**5a**), carnemycin E (**5b**), acetyl carnemycin E (**5c**), tajixanthone hydrate (**6a**), 15-acetyl tajixanthone hydrate (**6b**).

2. Results and Discussion

The structures of *p*-hydroxybenzaldehyde (**1**) [9], 1,3-dimethoxy-8-hydroxy-6-methylanthraquinone (**3a**) [10], 1,3-dimethoxy-2,8-dihydroxy-6-methylanthraquinone (**3b**) [11], emodin (**3c**) [12], 5[(3*E*,5*E*)-nona-3,5-dien-1-yl]benzene-1,3-diol (**5a**) [13], carnemycin E (**5b**) [13], tajixanthone hydrate (**6a**) [14,15], and 15-acetyl tajixanthone hydrate (**6b**) [16] were elucidated by the analysis of their 1D and 2D NMR spectra as well as HRMS data (Figures S1, S2, S9–23, S29–S38, S47–S56, S59 and S60, Tables S1–S3) and by the comparison of their NMR spectral data with those reported in the literature.

Compound **2** was isolated as white crystals (mp 116–118 °C), and its molecular formula $C_{11}H_{12}O_5$ was established based on the (+)-HRESIMS *m/z* 225.0765 $[M + H]^+$ (calculated for $C_{11}H_{13}O_5$, 225.0763) (Figure S57), requiring six degrees of unsaturation. The ^{13}C NMR spectrum (Table 1, Figure S4), exhibited eleven carbon signals, which in combination with DEPT and HSQC spectra (Figure S6), can be categorized as one conjugated ester carbonyl (δ_C 169.1), two oxygen-bearing non-protonated sp^2 (δ_C 166.2 and 164.5), two non-protonated sp^2 (δ_C 142.1 and 100.0), two protonated sp^2 (δ_C 106.8 and 101.3), two oxymethine sp^3 (δ_C 77.8 and 67.5), one methoxy (δ_C 55.8) and one methyl (δ_C 15.9) carbon, respectively. The ^1H NMR spectrum (Table 1, Figure S3), in combination with the HSQC spectrum (Figure S6), displayed a singlet of the hydrogen-bonded hydroxyl proton at δ_H 11.20 (OH-8), a multiplet of a hydroxyl proton at δ_H 2.28 (OH-4), two doublets of meta-

coupled aromatic protons at δ_H 6.48 (J = 2.3 Hz, H-5/δ_C 106.8) and δ_H 6.45 (J = 2.3 Hz, H-7/δ_C 101.3), a double quartet at δ_H 4.63 (J = 6.6, 2 Hz, H-3/δ_C 77.8), which was coupled with a double doublet at δ_H 4.50 (J = 5.6, 1.5 Hz, H-4/δ_C 67.5), a methoxy singlet at δ_H 3.85 (δ_C 55.8) and a methyl doublet at δ_H 1.55 (J = 6.6 Hz, Me-9/δ_C 15.9). The HMBC spectrum (Table 1, Figure S7) exhibited correlations from OH-8 to the carbons at δ_C 164.5 (C-8), 101.3 (C-7) and 100.0 (C-8a), H-5 to the carbons at δ_C 166.2 (C-6), C-7, C-8a, C-4, H-7 to C-5, C-6, C-8a, H-3 to Me-9, H-4 to C-4a (δ_C 142.1), C-5, C-8a, OMe-6 to C-6, Me-9 to C-3, C-4, and a weak correlation from OH-4 to C-3 and C-4.

**Table 1.** ^{1}H and ^{13}C NMR data (CDCl$_3$, 300 and 75 MHz), COSY, HMBC, and NOESY for **2**.

Position	δ_C, Type	δ_H, (J in Hz)	COSY	HMBC	NOESY
1	169.1, CO	-			
3	77.8, CH	4.63, dq (6.6, 2.0)	CH$_3$-9	CH$_3$-9	CH$_3$-9
4	67.5, CH	4.50, dd (5.6, 1.5)	OH-4	C-4a, 5, 8a	H-5, CH$_3$-9
4a	142.1, C	-	-		
5	106.8, CH	6.48, d (2.3)	H-7	C-4, 6, 7, 8a	H-4, OCH$_3$-6
6	166.2, C	-			
7	101.3, CH	6.45, d (2.3)	H-5,	C-5, 6, 8a	OCH$_3$-6
8	164.5, C	-			
8a	100.0, C	-			
9	15.9, CH$_3$	1.55, d (1.6)	H-3	C-3, 4	H-3, 4
OCH$_3$-6	55.8, CH$_3$	3.85, s		C-6	
OH-4	-	2.28, m		C-3, 4	
OH-8	-	11.20, s		C-7, 8, 8a	

The ^{1}H and ^{13}C NMR chemical shift values, together with COSY and HMBC correlations, revealed that the planar structure of **2** is the same as that of the enantiomeric mixture of (3*R*,4*R*)- and (3*S*,4*S*)-4-hydroxy-6-methoxymellein, previously isolated from the culture extract of the mycobionts of *Graphis* sp. Since the mixture showed a negative sign of Cotton effect at 267 nm, the authors proposed that the (3*R*,4*R*)-enantiomer was predominant [17]. Surprisingly, the NOESY spectrum (Table 1, Figure S8) of **2** exhibited a strong correlation from H-4 to Me-9, but not from H-3 to H-4, suggesting that H-4 and Me-9 are on the same face, which is contrary to (3*R*,4*R*)- and (3*S*,4*S*)-4-hydroxy-6-methoxymellein where H-3 and H-4 are on the same face.

The absolute configurations of C-3 and C-4 were thus determined by comparison of the experimental ECD spectrum with a quantum-mechanically simulated spectrum derived from the most significant conformations of the computational models of (3*S*,4*R*)-**2** and (3*R*,4*S*)-**2** (Figure 2). Figure 3 shows a very good match between the experimental ECD spectrum and the calculated ECD spectrum for (3*S*,4*R*)-**2**, thus confirming that **2** is (3*S*,4*R*)-4-hydroxy-6-methoxymellein. Compound **2** is, therefore, a diastereomer of (3*R*,4*R*)- and (3*S*,4*S*)-4-hydroxy-6-methoxymellein [17] and has never been previously reported.
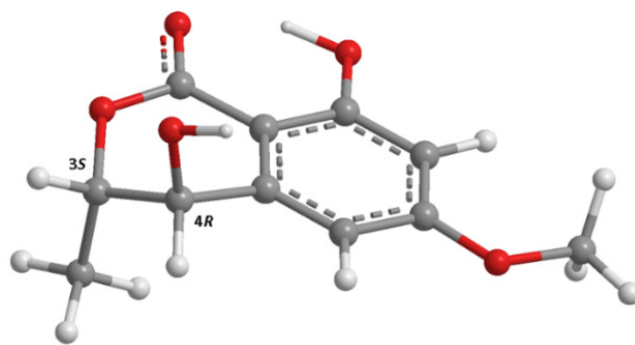
Figure 2. Model of the most abundant conformation of **2** (lowest APFD/6-311+G(2d,p)/acetonitrile energy conformer), accounting for 25% of conformer population, in its ECD-assigned (3*S*,4*R*) configuration.
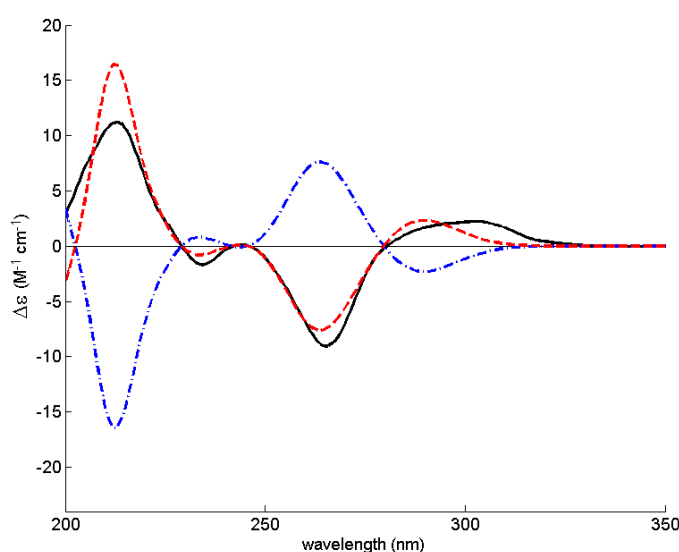
Figure 3. Experimental acetonitrile ECD spectrum of **2** (solid black line) and theoretical ECD spectra of its (3*R*,4*S*) (dot-dashed blue line) and (3*S*,4*R*) (dashed red line) computational models. Of the two theoretical spectra, the (3*R*,4*S*) was the one actually simulated and the (3*S*4,*R*) was obtained by changing the sign of every point of the (3*R*,4*S*) spectrum.

Compound **4** was isolated as a red solid (mp. 228–229 °C), and its molecular formula $C_{23}H_{19}NO_5$ was established on the basis of (+)-HRESIMS *m/z* 390.1340 [M + H]$^+$ (calculated for $C_{23}H_{20}NO_5$, 390.1341) (Figure S58), requiring fifteen degrees of unsaturation. The ^{13}C NMR spectrum (Table 2, Figure S25) displayed 23 carbon signals which, in combination with DEPT and HSQC spectra (Figure S27), can be classified as two conjugated ketone carbonyls (δ_C 184.5 and 183.3), three oxygen-bearing non-protonated sp^2 (δ_C 171.9, 161.2, 159.5), seven non-protonated sp^2 (δ_C 146.7, 142.8, 134.4, 133.2, 123.2, 114.6, 100.0), seven protonated sp^2 (δ_C 147.2, 146.2, 145.6, 127.5, 124.4, 120.4, and 118.6), two methylene sp^3 (δ_C 33.8 and 23.7), and two methyl (δ_C 21.9 and 13.7) carbons. The ^1H NMR spectrum (Table 2, Figure S24) showed two singlets of hydrogen-bonded phenolic hydroxyls at δ_H 12.50 and 13.44, seven aromatic protons appearing as a broad singlet at δ_H 8.91, two singlets at δ_H 7.11 and 6.80, three doublets at δ_H 8.57 (*J* = 8.0 Hz), 8.85 (*J* = 6.1 Hz), 7.46 (*J* = 1.0 Hz), one double doublet at δ_H 8.16 (*J* = 8.0, 6.1 Hz), one methylene triplet at δ_H 2.83 (*J* = 7.4 Hz), one methylene sextet at δ_H 1.70 (*J* = 7.4 Hz), one methyl singlet at δ_H 2.40, and one methyl triplet at δ_H 0.94 (*J* = 7.3 Hz). The presence of the 1,8-dihydroxy-6-methyl-1,2,3,6,8-pentasubstitututed anthraquinone scaffold was supported by COSY correlations (Table 2, Figures 4 and S26) from H-7 (δ_H 7.11, s/δ_C 124.4) to H-5 (7.46, d, *J* = 1.0 Hz)/δ_C 120.4) and Me-11 (2.40, s/δ_C 21.9), as well as by HMBC correlations (Table 2, Figures 4 and S28) from OH-1 (δ_H 13.44, s) to C-1 (δ_C 159.5), C-2 (δ_C 123.2), C-9a (δ_C 100.0), OH-8 (δ_H 12.50, s) to C-7 (δ_C 124.4), C-8

(δ_C 161.2), C-8a (δ_C 114.6), H-5 (δ_H 7.46, d, *J* = 1.0 Hz) to C-10 (δ_C 183.3), C-7, C-8a, Me-11 (δ_C 21.9), H-7 (δ_H 7.11, s) to C-8, C-5 (δ_C 120.4), C-8a, Me-11, H-4 (δ_H 6.80,s) to C-10, C-2 (δ_C 123.2), and C-9a. That another portion of the molecule is 3-propylpyridinium was corroborated by COSY correlations (Table 2, Figures 4 and S26) from H-4′ (δ_H 8.57, d, *J* = 8.0 Hz) to H-5′ (δ_H 8.16, dd, *J* = 8.0, 6.1 Hz) and H-2′ (δ_H 8.91, brs), H-5′ to H-4′ and H-6′ (8.85, d, *J* = 6.1 Hz), which was confirmed by HMBC correlations (Table 2, Figures 4 and S28) from H-2′ to C-3′ (δ_C 142.8), C-4′ (δ_C 146.2) and C-1″ (δ_C 33.8), H-4′ to C-2′ (δ_C 147.2), C-6′ (δ_C 145.6) and C-1″, H-5′ to C-3′, and C-6′ and H-6′ to C-4′ and C-5′ [18]. That the propyl group was on C-3′ of the pyridinium ring was supported by the spin system from H_2-1″ (δ_H 2.83, t, *J* = 7.4 Hz/δ_C 33.8) through H_2-2″ (δ_H 1.70, sex, *J* = 7.4 Hz/δ_C 23.7) to H_3-3″ (δ_H 0.94, t, *J* = 7.4 Hz/δ_C 13.7) as well as by HMBC correlations from H-3″ to C-1″ and C-2″, H-2″ to C-1″, and C-3″ and C-2′. Since H-2′ and H-6′ showed strong and weak cross peaks, respectively, to C-2 (Table 2, Figures 4 and S28), the 3-propylpyridinium moiety is linked to the anthraquinone scaffold through the nitrogen atom for the former and C-2 of the latter.

Table 2. ^{1}H and ^{13}C NMR data (DMSO-d_6, 500 and 125 MHz), COSY and HMBC assignment for **4**.

| Position	δ_C, Type	δ_H, (*J* in Hz)	COSY	HMBC
1	159.5, C			
2	123.2, C			
3	171.9, C			
4	118.6, CH	6.80, s		C-2, 9a, 10
4a	133.2, C			
5	120.4, CH	7.46, d (1.0)	H-7	C-7, 8a, 10, CH$_3$-11
6	146.7, C			
7	124.4, CH	7.11, s	H-5, CH$_3$-11	C-5, 8, 8a, CH$_3$-11
8	161.2, C			
8a	114.6, C			
9	184.5, CO			
9a	100.0, C			
10	183.3, CO			
10a	134.4, C			
11	21.9, CH$_3$	2.40, s	H-7	C-5, 6,7
2′	147.2, CH	8.91, brs	H-4′	C-2, 3′, 4′, 1″
3′	142.8, C			
4′	146.2, CH	8.57, d (8.0)	H-2′,5′	C-2′, 6′, 1″
5′	127.5, CH	8.16, dd (8.0, 6.1)	H-4′, 6′	C-3′, 6′
6′	145.6, CH	8.85, d (6.1)	H-5′	C-2, 4′, 5′
1″	33.8, CH$_2$	2.83, t (7.4)	H-2″	C-2′, 2″, 3′, 3″
2″	23.7, CH$_2$	1.70, sex (7.4)	H-1″, 3″	C-1″, 3′, 3″
3″	13.7, CH$_3$	0.94, t (7.3)	H-2″	C-1″, 3″
OH-1		13.44, s		C-1, 2, 9a
OH-8		12.50, s		C-7, 8, 8a
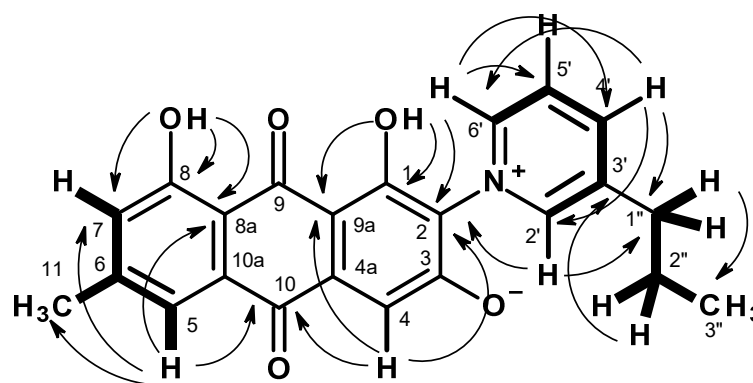
Figure 4. Key COSY (——) and HMBC (⌒) correlations in **4**.

Since 1,8-dihydroxy-6-methyl anthraquinone and the 3-propylpyridinium moiety account for $C_{23}H_{19}NO_4$, the only oxygen atom left must be on C-3 of the anthraquinone nucleus to produce a molecular formula $C_{23}H_{19}NO_5$. Therefore, the oxygen atom on C-3 should bear a negative charge (**4**). This was supported by a high chemical shift value of C-3 (δ_C 171.9). This phenoxide ion can establish an ionic interaction with the positive-charged nitrogen of the pyridinium ring. Interestingly, although alkyl pyridinium-containing compounds have never been reported from marine-derived fungi, cyclic 3-alkylpyridinium alkaloids are common secondary metabolites from sponges of the order Haplosclerida [19,20]. Therefore, **4** is the first 3-alkylpyridinium anthraquinone reported from nature, and it was named stellatanthraquinone.

Compound **5b** was isolated as a pale-yellow viscous mass, and its molecular formula $C_{21}H_{30}O_7$ was established on the basis of the (+)-HRESIMS *m/z* 395.2076 [M + H]⁺ (calculated for $C_{21}H_{31}O_7$, 395.2070 (Figure S60), requiring seven degrees of unsaturation. Analysis of its ¹H, ¹³C NMR, DEPT, COSY, HSQC, and HMBC spectra (Table 3, Figures S34–S38) revealed the presence of a 5 [(3*E*,5*E*)-nona-3,5-dien-1-yl]benzene-1,3-diol moiety, identical to **5a**, with a substitution on C-2. The presence of five oxymethine sp³ (δ_C 81.5, 79.1, 75.0, 72.1, 70.3), one oxymethylene sp³ (δ_C 61.2) carbons, two hydroxyl groups at δ_H 4.90 dd (*J* = 10.7, 2.9 Hz) and 4.59 d (*J* = 5.5 Hz), and the molecular formula $C_6H_{11}O_5$ of the substituent on C-2 revealed the presence of a pyranosyl moiety. However, since four oxymethine protons of the sugar moiety appeared as complex multiplets at δ_H 3.20–3.22 and 3.74, it was not possible to identify the sugar moiety of **5b**. Although Wen et al. [13] identified the sugar moiety in carnemycin E as glucopyranosyl, it was not possible to compare its ¹H and ¹³C chemical shift values with those of the sugar moiety **5b** since the ¹H and ¹³C NMR spectra of carnemycin E were obtained in pyridine-*d5*, while those of **5b** were obtained in DMSO-*d6*. Moreover, carnemycin E was obtained as an amorphous reddish gum, while **5b** was obtained as a pale-yellow viscous mass. In order to unravel the identity of the sugar moiety in **5b**, we tried to compare its carbon chemical shift values with those of the C-glycosides from the ¹³C NMR spectra obtained in DMSO-*d6*. The chemical shift values of C-1′, C-2′, C-3′, C-4′, C-5′ and C-6′ of the sugar moiety of **5b** (Table 3, Figure S36) were nearly identical to those of C-glucosyl moiety of tricetin 6,8-di-C-glucoside [21]. Moreover, the chemical shift value and coupling constant of H-1′ were also identical with those of the corresponding proton in tricetin 6,8-di-C-glucoside [21]. The value of the coupling constant of H-1′ (*J* = 9.6 Hz) confirmed the presence of a β-D-glucopyranosyl moiety. Therefore, **5a** was elucidated as carnemycin E, previously isolated from the culture extract of *Aspergillus* sp., which was isolated from superficial mycobiota of the brown alga, *Saccharina cichorioides* f. *sachalinensis,* collected from the South China Sea [13].

Table 3. ^{1}H and ^{13}C NMR data (DMSO-d_6, 300 and 75 MHz), COSY, and HMBC assignment for **5b**.

Position	δ_C, Type	δ_H, (J in Hz)	COSY	HMBC
1	157.1, C			
2	110.2, C			
3	157.1, C			
4	107.6, CH	6.11, s		C-1′, 3, 6, 7
5	142.5, C			
6	107.6, CH	6.11, s		C-1′, 2, 4, 7
7	35.5, CH$_2$	2.45, t (6.8)	H-8	C-4, 5, 6, 8, 9
8	34.0, CH$_2$	2.27, dd (14.3, 6.6)	H-7, H-9	C-5, 7, 9, 10
9	131.8, CH	5.62, m	H-8, 10	C-10, 11
10	130.9, CH	5.91, m	H-9, 11	C-8, 9, 12
11	131.1, CH	6.04, m	H-10, 12	C-9, 13
12	132.6, CH	5.55, m	H-11, 13	C-10, 13, 14
13	34.5, CH$_2$	2.00, dd (14.3, 7.2)	H-12, 14	C-11, 12, 14, 15
14	22.5, CH$_2$	1.36, sext (7.2)	H-13, 15	C-12, 13, 15
15	14.0, CH$_3$	0.87, t (7.2)	H-14	C-13, 14
1′	75.0, CH	4.62, d (9.6)	H-2′	C-1, 2, 2′, 3, 3′
2′	72.1, CH	3.74, m		
3′	79.1, CH	3.22, m		
4′	70.3, CH	3.22, m	OH-4′	
5′	81.5, CH	3.20, m		
6′a b	61.2, CH$_2$	3.50, dd (11.0, 5.5) 3.65, dd (11.0, 5.2)	H-5′, 6′b, OH-6′ H-5′, 6′a, OH-6′	
OH-3		8.67, s		C-2, 3, 4
OH-4′		4.90, dd (10.7, 2.9)	H-4′	C-4′, 5′
OH-6′		4.59, d (5.5)	H$_2$-6′	C-6′

　　　　Compound **5c** was also isolated as a pale-yellow viscous mass and its molecular formula C$_{23}$H$_{32}$O$_8$ was established on the basis of the (+)-HRESIMS *m/z* at 437.2175 [M + H]$^+$ (calculated for C$_{23}$H$_{33}$O$_8$, 437.2175), and *m/z* 459.1989 [M + Na]$^+$ (calculated for C$_{23}$H$_{32}$O$_8$Na, 459.1995) (Figure S61).The ^{1}H and ^{13}C NMR spectra of **5c** (Table 4; Figures S39 and S40) resembled those of **5b** (Table S2 and Figures S34 and S35) except for CH$_2$-6′, which appeared at higher frequencies (δ_H 4.32 d, *J* = 11.6 Hz, and 3.98 dd, *J* = 11.6, 3.9 Hz/δ_C 64.8) than those of **5b** (δ_H 3.50, dd, *J* = 11.0, 5.5 Hz, and 3.65, dd, *J* = 11.0, 5.2 Hz)/δ_C 61.2) as well as the appearance of an acetyl group (δ_H 2.00, s/δ_C 21.2, CH$_3$; δ_C 170.9, CO), suggesting that **5c** is a C-21 acetate of **5b**.

　　　　Contrary to other proton signals, the signals of OH-3, OH-3′, and OH-4′ appeared as broad signals in the ^{1}H NMR spectrum at 500 MHz (Figure S39). Moreover, they did not show any COSY and HMBC correlations with any protons (Table 4, Figures S41 and S43), which made it impossible to assign them. Interestingly, in the ^{1}H NMR spectrum at 300 MHz (Figure S44), the signal of OH-3 appeared as a sharp singlet at δ_H 8.70, whereas those of OH-3′ and OH-4′ appeared as two well-resolved doublets at δ_H 4.59, d (*J* = 6.5 Hz) and 5.15, d (*J* = 4.4 Hz), respectively. Furthermore, in the 300 MHz spectra, OH-3 displayed HMBC correlations to C-2 (δ_C 109.9) and C-3 (δ_C 157.2) (Figure S46), while OH-3′ and OH-4′ showed COSY correlations to H-3′ (δ_H 3.20) and H-4′ (δ_H 3.18) (Figure S45), respectively.

The coupling constant of H-1' (*J* = 9.8 Hz) confirmed the β-anomer of the glucosyl moiety. Since **5c** has never been previously reported, it was named acetyl carnemycin E.

**Table 4.** ^{1}H and ^{13}C NMR data (DMSO-d_6, 500 and 125 MHz), COSY, and HMBC assignment for **5c**.

Position	δ_C, Type	δ_H, (*J* in Hz)	COSY	HMBC
1	157.3, C			
2	109.9, C			
3	157.3, C			
4	107.5, CH	6.11, s		C-1', 2, 3, 6, 7
5	142.5, C			
6	107.5, CH	6.11, s		C-1', 2, 3, 4, 7
7	35.5, CH$_2$	2.44, t (7.2)	H-8	C-4, 5, 6, 8, 9
8	34.0, CH$_2$	2.26, dd (14.7, 7.2)	H-7, 9	C-7, 9, 10
9	131.8, CH	5.59, ddd (14.6, 7.2, 7.2)	H-8, 10	C-11
10	130.9, CH	5.97, m	H-9, 11	
11	131.1, CH	6.04, m	H-10, 12	C-9 (w), 13
12	132.6, CH	5.57, ddd (14.5, 7.7, 7.1)	H-11, 13	C-10, 13, 14
13	34.5, CH$_2$	2.01, m	H-12, 14	C-11, 12, 14, 15
14	22.5, CH$_2$	1.36, sex (7.4)	H-13, 15	12, 13, 15
15	14.0, CH$_3$	0.86, t (7.4)	H-14	C-13, 14
1'	74.9, CH	4.60, d (9.8)	H-2'	C-1, 2, 2' 3, 3'
2'	71.5, CH	3.83, t (9.2)	H-1', 3'	C-1', 3'
3'	79.0, CH	3.21, t (8.7)	H-4'	C-4'
4'	70.6, CH	3.18, t (8.7)	H-3'	C-3'
5'	78.4, CH	3.36 (under water peak)	H-6'b	C-4' (w)
6'a b	64.8, CH$_2$	4.32, d (11.6) 3.98, dd (11.6, 3.9)	H-6'b H-5', 6'a	C-4', CO (OAc) C-5', 6'
OAc	170.9, CO	-		
OAc	21.2, CH$_3$	2.00, s		C-6'
OH-3		8.74, brs		
OH-3'		4.95, br		
OH-4'		5.15, br		

The ^{1}H and ^{13}C NMR spectra of **6a** and **6b** (Table S3. Figures S47, S48, S52 and S53) are in agreement with those reported for tajixanthone hydrate [14] and 15-acetyl tajixanthone hydrate [16]. However, Pornpakakul et al. [14] assigned the configurations of C-15, C-20 and C-25 of tajixanthone hydrate, based on the coupling constant between H-14 and H-15 and NOESY correlations of the protons in tajixanthone methanoate, and also referred its stereochemistry to the previous study by Chexal et al. [22], who elegantly determined the absolute configurations of C-15 and C-25 of tajixanthone as 15*S* and 25*R* by chemical transformation (the method of Boar and Damps) while the relative configuration of C-20 was suggested by the preferred axial conformation of the isopropyl substituent in the hydrogenated derivatives [22]. Later on, the same group [23], described the isolation of tajixanthone hydrate which they obtained in a small quantity. The structure and stereochemistry of tajixanthone hydrate were identified on the basis of the same optical rotation of the acid-catalyzed hydrolysis product of tajixanthone and of the natural product. On the other hand, the absolute stereochemistry of 15-acetyl tajixanthone hydrate was concluded

to be the same as that of tajixanthone hydrate, which was obtained by hydrolysis of 15-acetyl tajixanthone hydrate. However, neither optical rotation nor absolute configurations of their stereogenic carbons were provided [16].

Literature search revealed that the absolute configurations of C-15, C-20, and C-25 of both tajixanthone hydrate and 15-acetyl tajixanthone hydrate have never been established by either X-ray crystallographic or chiroptical methods. Fortunately, we were able to obtain suitable crystals of both **6a** and **6b** for X-ray analysis using an X-ray diffractometer equipped with CuKα radiation. The Ortep views of **6a** and **6b** are shown in Figures 5A and 5B, respectively, revealing that the absolute configurations of C-15, C-20, and C-25 in both compounds are 15*S*, 20*S*, and 25*R*. Moreover, both compounds are levorotatory.

(A)
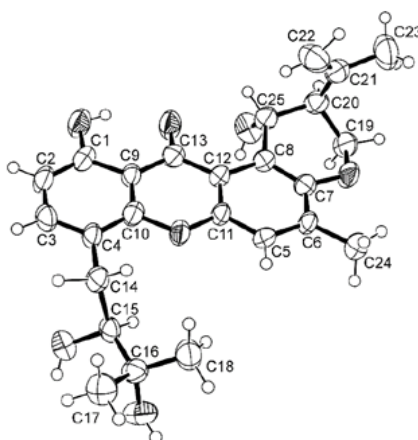
(B)
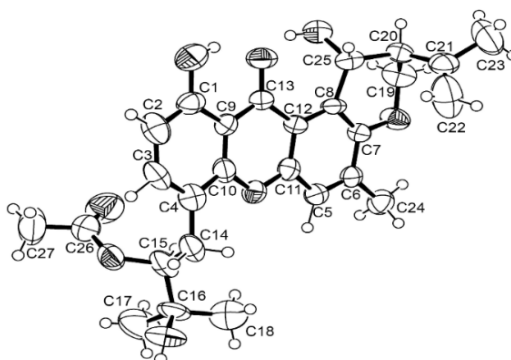
Figure 5. Ortep views of **6a** (**A**) and **6b** (**B**).

The antimicrobial activity of **2**, **3a**, **3b**, **4**, **5a**, **5b**, **5c**, **6a**, and **6b** was evaluated against four reference bacterial species and three multidrug-resistant strains. However, only **5a** exhibited antibacterial activity against all Gram-positive strains, viz. *E. faecalis* ATCC 29212, vancomycin-resistant *E. faecalis* B3/101, and methicillin-resistant *S. aureus* 74/24, with a MIC value of 16 µg/mL, and *S. aureus* ATCC 29213, with a MIC value of 32 µg/mL (Table 5). The minimal bactericidal concentration (MBC) for **5a** was equal to or one-fold higher than the MIC, indicating its bactericidal effect towards *E. faecalis* ATCC 29212, *S. aureus* 74/24, and *S. aureus* ATCC 29213. For *E. faecalis* B3/101, its MBC was more than two-fold higher than the MIC, suggesting its bacteriostatic effect.

Table 5. Antibacterial activity of **2**, **3a**, **3b**, **4**, **5a**, **5b**, **5c**, **6a**, and **6b** against Gram-positive reference and multidrug-resistant strains. MIC and MBC are expressed in μg/mL.

Compound	*E. faecalis* ATCC 29212		*E. faecalis* B3/101 (VRE)		*S. aureus* ATCC 29213		*S. aureus* 74/24 (MRSA)	
	MIC	MBC	MIC	MBC	MIC	MBC	MIC	MBC
2	>64	>64	>64	>64	>64	>64	>64	>64
3a	>32	>32	>32	>32	>32	>32	>32	>32
3b	>64	>64	>64	>64	>64	>64	>64	>64
4	>32	>32	>32	>32	>32	>32	>32	>32
5a	16	32	16	64	32	32	16	32
5b	>64	>64	>64	>64	>64	>64	>64	>64
5c	>64	>64	>64	>64	>64	>64	>64	>64
6a	>64	>64	>64	>64	>64	>64	>64	>64
6b	>32	>32	>32	>32	>32	>32	>32	>32
VAN	4	-	-	-	-	-	-	-
OXA	-	-	-	-	0.2	-	-	-

MIC, minimal inhibitory concentration; MBC, minimal bactericidal concentration; VAN, vancomycin; OXA, oxacillin.

Although **5a** was found to significantly inhibit NO production in lipopolysaccharide (LPS)-induced murine macrophage RAW264.7 cells [13], this compound has never been tested for antibacterial acivity. Interestingly, some alkenylresorcinols, such as 9-(3,5-dihydroxy-4-methylphenyl)nona-3(Z)-enoic acid, isolated from the methanolic extract of fruits of *Hakea sericea*, significantly inhibited the growth of *E. faecalis*, *Listeria monocytogenes* and *Bacillus cereus*, and showed good MIC values against *S. aureus* strains, including the clinical isolates and MRSA strains [24]. Intriguingly, **5b** and **5c**, analogs of **5a** which possess a β-glucosyl moiety on C-2 of the benzene ring, were void of antibacterial activity in our assays. We speculate that the polar and bulky glucosyl moiety might have negatively affected the antibacterial activity, possibly by preventing the compounds from penetrating the bacterial cell wall.

Another interesting aspect is that even though there were several reports on the antibaterial activity of anthraquinones from marine-derived fungi [25], neither of the three anthraquinones tested, i.e. **3a**, **3b**, and **4**, showed antibacterial activity in our assays. This is not surprising since we also found in our previous report that the anthraquinone purnipurdin A, isolated from the culture extract of the marine sponge-associated fungus, *Neosartorya spinosa* KUFA 1047, did not exhibit any antibacterial activity against the same bacterial strains tested [26].

Compounds **2**, **3a**, **3b**, **4**, **5a**, **5b**, **5c**, **6a,** and **6b** were also investigated for their potential synergy with clinically relevant antibiotics on multidrug-resistant strains, by both disk diffusion method and checkerboard assay; however, no interactions were found with cefotaxime (ESBL *E. coli*), methicillin (MRSA *S. aureus*), and vancomycin (VRE *E. faecalis*).

The inhibitory effect of **2**, **3a**, **3b**, **4**, **5a**, **5b**, **5c**, **6a**, and **6b** on biofilm production was also evaluated in all reference strains. However, only **5a** showed an extensive ability to significantly inhibit biofilm formation in two of the four reference strains used in this study (Table 6). Indeed, **5a** was able to completely inhibit biofilm formation in *S. aureus* ATCC 29213 and *E. faecalis* ATCC 29212, at both MIC and 2xMIC concentrations.

Table 6. Percentage of biofilm formation in the presence of **5a** after 24 h incubation.

Compound	Concentration	Biofilm Biomass (% of Control)	
		E. faecalis **ATCC 29212**	*S. aureus* **ATCC 29213**
5a	64 μg/mL	-	0.00 ± 0.06 ***
	32 μg/mL	0.01 ± 0.01 ***	0.04 ± 0.12 ***
	16 μg/mL	0.02 ± 0.01 ***	-
DMSO	1% (*v/v*)	1.00 ± 0.03 ***	1.00 ± 0.01 ***

Data are shown as mean ± SD of three independent experiments. One-sample *t*-test: * $p < 0.05$, ** $p < 0.01$, *** $p < 0.001$ significantly different from 100%.

3. Experimental Sections

3.1. General Experimental Procedures

The melting points were determined on a Stuart Melting Point Apparatus SMP3 (Bibby Sterilin, Stone, Staffordshire, UK) and are uncorrected. Optical rotations were measured on an ADP410 Polarimeter (Bellingham + Stanley Ltd., Tunbridge Wells, Kent, UK). ^{1}H and ^{13}C NMR spectra were recorded at ambient temperature on a Bruker AMC instrument (Bruker Biosciences Corporation, Billerica, MA, USA) operating at 300 or 500 and 75 or 125 MHz, respectively. High resolution mass spectra were measured with a Waters Xevo QToF mass spectrometer (Waters Corporations, Milford, MA, USA) coupled to a Waters Aquity UPLC system. A Merck (Darmstadt, Germany) silica gel GF$_{254}$ was used for preparative TLC, and a Merck Si gel 60 (0.2–0.5 mm) was used for column chromatography. LiChroprep silica gel and Sephadex LH 20 were used for column chromatography.

3.2. Fungal Material

The fungus was isolated from the marine sponge *Mycale* sp., which was collected by scuba diving at a depth of 5–10 m, from the coral reef at Samaesan Island (12°34′36.64″ N 100°56′59.69″ E), in the Gulf of Thailand, Chonburi province, in May 2015. The sponge was washed with 0.01% sodium hypochlorite solution for 1 min, followed by sterilized seawater three times, and then dried on a sterile filter paper under a sterile aseptic condition. The sponge was cut into small pieces (*ca.* 5 × 5 mm) and placed on Petri dish plates containing 15 mL potato dextrose agar (PDA) medium mixed with 300 mg/L of streptomycin sulfate and incubated at 28 °C for 7 days. The hyphal tips emerging from sponge pieces were individually transferred onto a PDA slant and maintained as pure cultures at Kasetsart University Fungal Collection, Department of Plant Pathology, Faculty of Agriculture, Kasetsart University, Bangkok, Thailand. The fungal strain KUFA 2017 was identified as *Aspergillus stellatus*, based on morphological characteristics such as colony growth rate and growth pattern on standard media, namely Czapek′s agar, Czapek yeast autolysate agar, and malt extract agar. Microscopic characteristics including size, shape, and ornamentation of conidiophores and spores were examined under light microscope. This identification was confirmed by molecular techniques using internal transcribed spacer (ITS) primers. DNA was extracted from young mycelia following a modified Murray and Thompson method [27]. Primer pairs ITS1 and ITS4 were used for ITS gene amplification [28]. PCR reactions were conducted on Thermal Cycler and the amplification process consisted of initial denaturation at 95 °C for 5 min, 34 cycles at 95 °C for 1 min (denaturation), at 55 °C for 1 min (annealing), and at 72 °C for 1.5 min (extension), followed by final extension at 72 °C for 10 min. PCR products were examined by Agarose gel electrophoresis (1% agarose with 1× Tris-Borate-EDTA (TBE) buffer) and visualized under UV light after staining with ethidium bromide. DNA sequencing analyses were performed using the dideoxyribonucleotide chain termination method [29] by Macrogen Inc. (Seoul, South Korea). The DNA sequences were edited using FinchTV software and submitted to the BLAST program for alignment and compared with that of fungal species in the NCBI database (http://www.ncbi.nlm.nih.gov/, accessed on 18 May 2021). Its gene sequences were deposited in GenBank with the accession number MZ331807.

3.3. Extraction and Isolation

The fungus was cultured in five Petri dishes (i.d. 90 mm) containing 20 mL of PDA per dish at 28 °C for one week. The mycelial plugs (5 mm in diameter) were transferred to two 500 mL Erlenmeyer flasks containing 200 mL of potato dextrose broth (PDB), and incubated on a rotary shaker at 120 rpm at 28 °C for one week. Thirty 1000 mL Erlenmeyer flasks, each containing 300 g of cooked rice, were autoclaved at 121 °C for 15 min. After cooling to room temperature, 20 mL of mycelial suspension of the fungus was inoculated per flask and incubated at 28 °C for 30 days, after which 500 mL of EtOAc was added to each flask of the moldy rice and macerated for 7 days, and then filtered with Whatman No. 1 filter paper.

The EtOAc solutions were combined and concentrated under reduced pressure to yield 280.4 g of a crude EtOAc extract, which was dissolved in 300 mL of $CHCl_3$, washed with H_2O (3 × 500 mL) and dried with anhydrous Na_2SO_4, and filtered and evaporated under reduced pressure to obtain 134.9 g of a crude $CHCl_3$ extract. The crude $CHCl_3$ extract (57.1 g) was applied on a silica gel column (385 g) and eluted with mixtures of petrol-$CHCl_3$ and $CHCl_3$-Me_2CO, wherein 250 mL fractions (frs) were collected as follows: frs 1–61 (petrol-$CHCl_3$, 1:1), 62–129 (petrol-$CHCl_3$, 3:7), 130–231 (petrol-$CHCl_3$, 1:9), 232–397 ($CHCl_3$-Me_2CO, 9:1), 398–524 ($CHCl_3$-Me_2CO, 7:3). Frs 40–45 were combined (241.9 mg) and applied over a Sephadex LH-20 column (15 g), and eluted with MeOH, wherein 37 subfractions (sfrs) of 2 mL were collected. Sfrs 30–35 were combined (102.9 mg) and precipitated in MeOH to produce 13.6 mg of **3a**. Frs 74–77 were combined (851.6 mg) and precipitated in Me_2CO to produce 20.3 mg of **3b**. Frs 78–89 were combined (396.5 mg) and applied over a Sephadex LH-20 column (15 g), and eluted with MeOH, wherein 28 sfrs of 2 mL were collected. Sfrs 21–25 were combined to produce 11.4 mg of **3c**. Frs 95–118 were combined (535.5 mg) and applied over a Sephadex LH-20 column (15 g), and eluted with MeOH, wherein 47 sfrs of 2 mL were collected. Sfrs 16–33 were combined (231.4 mg) and applied over another Sephadex LH-20 column (5 g), and eluted with $CHCl_3$, wherein 22 sub-subfractions (ssfrs) of 1 mL were collected. Ssfrs 9–10 were combined to produce 69.4 mg of **2**, while ssfrs 20–22 were combined to produce 45.0 mg of **1**. Frs 126–140 were combined (274.9 mg) and applied over a Sephadex LH-20 column (15 g), and eluted with MeOH, wherein 31 sfrs of 2 mL were collected. Sfrs 4–15 were combined (108.4 mg) and precipitated in Me_2CO to produce 26.7 mg of **6b**. Frs 149-173 were combined (1.02 g) and applied over a Sephadex LH-20 column (15 g), and eluted with MeOH, wherein 49 sfrs of 1 mL were collected. Sfrs 20–28 were combined (305.2 mg) and applied over another Sephadex LH-20 column (5 g), and eluted with $CHCl_3$, wherein 20 ssfrs of 0.5 mL were collected. Ssfrs 15–19 were combined to produce 153.0 mg of **5a**. Frs 178–206 were combined (509.4 mg) and precipitated in MeOH to produce 46.8 mg of **6a**. Frs 237–238 were combined (209.3 mg) and applied over a Sephadex LH-20 column (15 g), and eluted with MeOH, wherein 20 sfrs of 2 mL were collected. Sfrs14-20 were combined (182.4 g) and applied over another Sephadex LH-20 column (5 g), and eluted with $CHCl_3$, wherein 13 ssfrs of 1 mL were collected. Ssfrs 8–9 were combined to produce 7.3 mg of **5c**. Frs 437-455 were combined (323.3 mg) and applied over a Sephadex LH-20 column (15 g), and eluted with MeOH, wherein 24 sfrs of 2 mL were collected. Sfrs 11–15 were combined (211.9 mg) and applied over another Sephadex LH-20 column (5 g), and eluted with $CHCl_3$, wherein 18 ssfrs of 0.5 mL were collected. Ssfrs 17–18 were combined to produce 141.7 mg of **5b**. Frs 460–513 were combined (297.3 mg) and applied over a Sephadex LH-20 column (15g), and eluted with MeOH, wherein 25 sfrs of 2 mL were collected. Sfrs 15–18 were combined (20.9 mg) and applied over another Sephadex LH-20 column (5 g), and eluted with $CHCl_3$, wherein 13 ssfrs of 0.5 mL were collected. Ssfrs 4–7 were combined to produce 5.6 mg of **4**.

3.3.1. (3*S*,4*R*)-4-Hydroxy-6-Methoxymellein (**2**)

White crystal. Mp 116–118 °C. $[\alpha]_D^{23}$ −200 (*c* 0.05, MeOH); For ^1H and ^{13}C spectroscopic data (CDCl$_3$, 300 and 75 MHz), see Table 1; (+)-HRESIMS *m/z* 225.0765 [M + H]$^+$ (calculated for $C_{11}H_{13}O_5$, 225.0763).

3.3.2. Stellatanthraquinone (**4**)

Red solid. Mp. 228–229 °C. For ^{1}H and ^{13}C spectroscopic data (DMSO-*d6*, 500 and 125 MHz), see Table 2; (+)-HRESIMS *m/z* 390.1340 [M + H]$^+$ (calculated for $C_{23}H_{20}NO_5$, 390.1341).

3.3.3. Carnemycin E (**5b**)

Pale-yellow viscous mass. $[\alpha]^{20}_D$ +60 (*c* 0.05, MeOH). [1]H and ^{13}C spectroscopic data (DMSO-*d6*, 300 and 75 MHz), see Table 3; (+)-HRESIMS *m/z* 395.2076 [M + H]$^+$ (calculated for $C_{21}H_{331}O_7$, 395.2070).

3.3.4. Acetyl Carnemycin E (**5c**)

Pale-yellow viscous mass. $[\alpha]^{20}_D$ +260 (*c* 0.05, MeOH). [1]H and ^{13}C spectroscopic data (DMSO-*d6*, 500 and 125 MHz), see Table 4; (+)-HRESIMS *m/z* 437.2175 [M + H]$^+$, (calculated for $C_{23}H_{33}O_8$, 437.2175); *m/z* 459.1989 [M + Na]$^+$ (calculated for $C_{23}H_{32}O_8Na$, 459.1995).

3.4. X-ray Crystal Structures

Single crystals were mounted on cryoloops using paratone. X-ray diffraction data were collected at 290 K with a Gemini PX Ultra equipped with CuK$_\alpha$ radiation (λ = 1.54184 Å). The structures were solved by direct methods using SHELXS-97 and refined with SHELXL-97 [30]. Non-hydrogen atoms were refined anisotropically. Hydrogen atoms were either placed at their idealized positions using appropriate HFIX instructions in SHELXL and included in subsequent refinement cycles or were directly found from difference Fourier maps and were refined freely with isotropic displacement parameters.

3.4.1. X-ray Crystal Structure of **6a**

Crystal was orthorhombic, space group $P2_12_12_1$, cell volume 2178.1(4) Å^3 and unit cell dimensions *a* = 6.2933(5) Å, *b* = 17.9862(18) Å and *c* = 19.243(3) Å (uncertainties in parentheses). Flack *x* [31] was refined parameter by means of TWIN and BASF in SHELXL to 0.0(5). The refinement converged to R (all data) = 8.88% and wR2 (all data) = 17.80%. Full details of the data collection and refinement and tables of atomic coordinates, bond lengths and angles, and torsion angles have been deposited with the Cambridge Crystallographic Data Centre (CCDC 2206108).

3.4.2. X-ray Crystal Structure of **6b**

The crystal was orthorhombic, space group P2$_1$2$_1$2$_1$, cell volume 2454.0(4) Å^3, and unit cell dimensions *a* = 5.9772(6) Å, *b* = 13.8321(13) Å and *c* = 29.682(2) Å (uncertainties in parentheses). Calculated crystal density was 1.306 g/cm^{-3}. The structure was solved by direct methods using SHELXS-97 and refined with SHELXL-97 [30]. The refinement converged to R (all data) = 8.45% and wR2 (all data) = 12.84% and Flack parameter = 0.0(3). Full details of the data collection and refinement and tables of atomic coordinates, bond lengths and angles, and torsion angles have been deposited with the Cambridge Crystallographic Data Centre (CCDC 2204631).

3.5. Electronic Circular Dichroism (ECD)

The experimental ECD spectrum of **2** (*ca.* 2 mg/mL in acetonitrile) was obtained in a Jasco J-815 CD spectropolarimeter (Jasco Europe S.R.L., Cremella, Italy) with a 0.1 mm cuvette and 6 accumulations. The simulated ECD spectra were obtained by first determining all the relevant conformers of the computational model. Its conformational space was developed by rotating all the single, non-ring, bonds for each of the two possible bends of the non-aromatic ring. The resulting 24 molecular mechanics conformers were minimized using the quantum mechanical DFT method B3LYP/6-31G with Gaussian 16W (Gaussian Inc., Wallingford, USA). The lowest 95% of the conformer Boltzmann populations (11 models) were subjected to a final minimization round using the method APFD/6-311+G(2d,p)/acetonitrile method (Gaussian 16W), which was also used, coupled with a TD method, to calculate its first 50 ECD transitions. The line spectrum for each one of the

11 models was built by applying a Gaussian line broadening of 0.15 eV to each computed transition with a constant UV-shift of 5 nm. The final ECD spectrum was obtained by the Boltzmann-weighted sum of the 11 line spectra [32].

3.6. Antibacterial Activity Bioassays

3.6.1. Bacterial Strains and Testing Conditions

Four reference strains, obtained from the American Type Culture Collection (ATCC), viz. two Gram-positive (*Staphylococcus aureus* ATCC 29213, *Enterococcus faecalis* ATCC 29212), and two Gram-negative (*Escherichia coli* ATCC 25922, *Pseudomonas aeruginosa* ATCC 27853), were included in this study. Additionally, three multidrug-resistant strains including an extended-spectrum β-lactamase (ESBL)-producing *E. coli* (clinical isolate SA/2), and two environmental isolates, i.e., a methicillin-resistant isolate (MRSA) *S. aureus* 74/24 [33], and a vancomycin-resistant (VRE) isolate *E. faecalis* B3/101 [34]. All bacterial strains were cultured in MH agar (MH-BioKar Diagnostics, Allone, France) and incubated overnight at 37 °C before each assay. Stock solutions of each compound (4 mg/mL for the less soluble compounds, **3a** and **4**, and 10 mg/mL for the others) were prepared in dimethyl sulfoxide (DMSO-Alfa Aesar, Kandel, Germany), kept at −20 °C, and freshly diluted in the appropriate culture media before each assay. In all experiments, in-test concentrations of DMSO were kept below 1%, as recommended by the Clinical and Laboratory Standards Institute [35].

3.6.2. Antimicrobial Susceptibility Testing

The Kirby–Bauer method was performed to screen the antimicrobial activity of the compounds according to CLSI recommendations [36]. Briefly, sterile blank paper discs with 6 mm diameter (Oxoid/Thermo Fisher Scientific, Basingstoke, UK) were impregnated with 15 μg of each compound and placed on MH plates, previously inoculated with a bacterial inoculum equal to 0.5 McFarland turbidity. After 18–20 h incubation at 37 °C, the diameter of the inhibition zones was measured in mm. Blank paper discs impregnated with DMSO were used as a negative control. Minimal inhibitory concentrations (MIC) were determined by the broth microdilution method, as recommended by the CLSI [37]. Two-fold serial dilutions of the compounds were prepared in cation-adjusted Mueller–Hinton broth (CAMHB-Sigma-Aldrich, St. Louis, MO, USA). With the exception of **3a** and **4**, the tested concentrations ranging from 1 to 64 μg/mL were used to keep in-test concentrations of DMSO below 1% to avoid bacterial growth inhibition. For **3a** and **4**, the highest concentration tested was 32 μg/mL. Colony forming unit (CFU) counts of the inoculum were conducted to ensure that the final inoculum size closely approximated the 5×10^5 CFU/mL. The 96-well U-shaped untreated polystyrene plates were incubated for 16–20 h at 37 °C, and the MIC was determined as the lowest concentration of the compound that prevented visible growth. During the essays, vancomycin (VAN-Oxoid/Thermo Fisher Scientific, Basingstoke, UK) and oxacillin sodium salt monosulfate (OXA-Sigma-Aldrich, St. Louis, MO, USA) were used as positive controls for *E. faecalis* ATCC 29212 and *S. aureus* ATCC 29213, respectively. The minimal bactericidal concentration (MBC) was determined by spreading 10 μL of the content of the wells with no visible growth on MH plates. The MBC was defined as the lowest concentration to effectively reduce 99.9% of the bacterial growth after overnight incubation at 37 °C [38]. At least three independent assays were conducted for reference and multidrug-resistant strains.

3.6.3. Antibiotic Synergy Testing

The Kirby–Bauer method was also used to evaluate the combined effect of the tested compounds with clinically relevant antibacterial drugs, as previously described [39]. A set of antibiotic discs (Oxoid/Thermo Fisher Scientific, Basingstoke, UK), to which the isolates were resistant, was selected: cefotaxime (CTX, 30 μg) for *E. coli* SA/2, vancomycin (VAN, 30 μg) for *E. faecalis* B3/101, and oxacillin (OXA, 1 μg) for *S. aureus* 74/24. Antibiotic discs impregnated with 15 μg of each compound were placed on seeded MH plates. The

controls used included antibiotic discs alone, blank paper discs impregnated with 15 μg of each compound alone, and blank discs impregnated with DMSO. Plates with CTX were incubated for 18–20 h and plates with VAN and OXA were incubated for 24 h at 37 °C [35]. Potential synergy was considered when the inhibition halo of the antibiotic disc impregnated with compound was greater than the inhibition halo of the antibiotic or compound-impregnated blank disc alone.

The MIC method was also performed in order to evaluate the combined effect of the compounds and clinically relevant antimicrobial drugs. Briefly, when it was not possible to determine a MIC value for the tested compound, the MIC of CTX (Duchefa Biochemie, Haarlem, The Netherlands), VAN (Oxoid, Basingstoke, England), and OXA (Sigma-Aldrich, St. Louis, MO, USA) for the respective multidrug-resistant strains was determined in the presence of the highest concentration of each compound tested in previous assays (64 μg/mL or 32 μg/mL for compounds **3a** and **4**). The tested antibiotic was serially diluted whereas the concentration of each compound was kept fixed. Antibiotic MICs were determined as described above. Potential synergy was considered when the antibiotic MIC was lower in the presence of compound [40]. Fractional inhibitory concentrations (FIC) were calculated as follows: FIC of the compound = MIC of the compound combined with antibiotic/MIC of the compound alone, and FIC antibiotic = MIC of antibiotic combined with compound/MIC of antibiotic alone. The FIC index (FICI) was calculated as the sum of each FIC and interpreted as follows: FICI ≤ 0.5, 'synergy'; 0.5 < FICI ≤ 4, 'no interaction'; 4 < FICI, 'antagonism' [41].

3.6.4. Biofilm Formation Inhibition Assay

In order to evaluate the antibiofilm activity of the compounds, the crystal violet method was used to quantify the total biomass produced [39,42]. Briefly, the highest concentration of the compound tested in the MIC assay was added to bacterial suspensions of 1×10^6 CFU/mL prepared in unsupplemented Tryptone Soy broth (TSB-Biokar Diagnostics, Allone, Beauvais, France) or TSB supplemented with 1% (*w/v*) glucose (D-(+)-glucose anhydrous for molecular biology, PanReac AppliChem, Barcelona, Spain) for Gram-positive strains. When it was possible to determine the MIC, concentrations between 2× MIC and 1/4 MIC were tested, while keeping in-test concentrations of DMSO below 1%. When it was not possible to determine the MIC value, the concentration tested was 64 μg/mL (or 32 μg/mL for compounds **3a** and **4**). Controls with appropriate concentration of DMSO, as well as a negative control (TSB or TSB + 1% glucose alone) were included. Sterile 96-well flat-bottomed untreated polystyrene microtiter plates were used. After a 24 h incubation at 37 °C, the biofilms were heat-fixed for 1 h at 60 °C and stained with 0.5% (*v/v*) crystal violet (Química Clínica Aplicada, Amposta, Spain) for 5 min. The stain was resolubilized with 33% (*v/v*) acetic acid (Acetic acid 100%, AppliChem, Darmstadt, Germany) and the biofilm biomass was quantified by measuring the absorbance of each sample at 570 nm in a microplate reader (Thermo Scientific Multiskan® FC, Thermo Fisher Scientific, Waltham, MA, USA). The background absorbance (TSB or TSB + 1% glucose without inoculum) was subtracted from the absorbance of each sample and the data are presented as percentage of control. Three independent assays were performed for reference strains, with triplicates for each experimental condition.

4. Conclusions

The EtOAc extract of the culture of a marine-derived fungus, *Aspergillus stellatus* KUFA 2017, isolated from a marine sponge *Mycale* sp., which was collected in the Gulf of Thailand, furnished three previously unreported secondary metabolites viz. (3*S*,4*R*)-4-hydroxy-6-methoxymellein (**2**), a structurally unique propylpyridinium anthraquinone, stellatanthraquinone (**4**), and acetyl carnemycin E (**5c**), in addition to eight previously reported compounds, including *p*-hydroxybenzaldehyde (**1**), 1,3-dimethoxy-8-hydroxy-6-methylanthraquinone (**3a**), 1,3-dimethoxy-2,8-dihydroxy-6-methylanthraquinone (**3b**), emodin (**3c**), 5[(3*E*,5*E*)-nona-3,5-dien-1-yl]benzene (**5a**), carnemycin E (**5b**), tajixanthone

hydrate (**6a**), and 15-acetyl tajixanthone hydrate (**6b**). While the absolute configurations of the stereogenic carbons in **2** were established unambiguously by a combination of NOESY correlations and a comparison of experimental and calculated ECD spectra, the stereostructures of **6a** and **6b** were established by X-ray analysis for the first time.

All the compounds, except **1** and **3c**, were evaluated for their antibacterial activity against four reference strains: two Gram-positive (*Staphylococcus aureus* ATCC 29213, *Enterococcus faecalis* ATCC 29212) and two Gram-negative (*Escherichia coli* ATCC 25922, *Pseudomonas aeruginosa* ATCC 27853), as well as three multidrug-resistant strains including an extended-spectrum β-lactamase (ESBL)-producing *E. coli* (clinical isolate SA/2), a methicillin-resistant isolate (MRSA) *S. aureus* 74/24 and a vancomycin-resistant (VRE) isolate *E. faecalis* B3/101. However, only **5c** exhibited antibacterial activity against all Gram-positive strains with a MIC value of 16 μg/mL toward *E. faecalis* ATCC 29212, vancomycin-resistant *E. faecalis* B3/101, and methicillin-resistant *S. aureus* 74/24, but with a higher MIC value (32 μg/mL) toward *S. aureus* ATCC 29213. Since **5a** displayed the minimal bactericidal concentration (MBC) equal to or one-fold higher than the MIC, it was suggested that **5a** exerted a bactericidal effect towards *E. faecalis* ATCC 29212, *S. aureus* 74/24, and *S. aureus* ATCC 29213. On the contrary, the MBC of **5a** was more than two-fold higher than the MIC toward *E. faecalis* B3/101; therefore, this compound was suggested to have a bacteriostatic effect against this multidrug-resistant species. Interestingly, **5b** and **5c**, which are C-glucosylated **5a**, were void of antibacterial activity against all the tested organisms. These results lead to a conclusion that the polar and bulky glucosyl substituent on the benzene ring can negatively affect the antibacterial activity of this series of compounds. Finally, **5a** was also able to completely inhibit biofilm formation in *S. aureus* ATCC 29213 and *E. faecalis* ATCC 29212 at both MIC and 2× MIC concentrations. Since **5a** possesses interesting antibacterial and potent antibiofilm activities, this compound can be considered as an interesting model for the development of a new type of antibiotics.

References

1. Wang, X.-C.; Zhuang, W.-Y. New species of *Aspergillus* (Aspergillaceae) from tropical islands of China. *J. Fungi* **2022**, *8*, 225. [CrossRef] [PubMed]

2. Hagestad, O.C.; Andersen, J.H.; Altermark, B.E.; Rämä, T. Cultivable marine fungi from the Arctic Archipelago of Svalbard and their antibacterial activity. *Mycology* **2020**, *11*, 230–242. [CrossRef] [PubMed]

3. Machado, F.P.; Kumla, D.; Pereira, J.A.; Sousa, E.; Dethoup, T.; Freitas-Silva, J.; Costa, P.M.; Mistry, S.; Silva, A.M.S.; Kijjoa, A. Prenylated phenylbutyrolactones from cultures of a marine sponge-associated fungus *Aspergillus flavipes* KUFA1152. *Phytochemistry* **2021**, *185*, 112709. [CrossRef] [PubMed]

4. Wang, Y.-T.; Xue, Y.-R.; Liu, C.-H. A brief review of bioactive metabolites derived from deep-sea fungi. *Mar. Drugs* **2015**, *13*, 4594–4616. [CrossRef]

5. Samson, R.; Visagie, C.M.; Houbraken, J.; Hong, S.B.; Hubka, V.; Klaassen, C.H.W.; Perrone, G.; Seifert, K.A.; Susca, A.; Tanney, J.B.; et al. Phylogeny, identification and nomenclature of the genus *Aspergillus*. *Stud. Mycol.* **2014**, *78*, 141–173. [CrossRef] [PubMed]

6. Orfali, R.; Aboseada, M.A.; Abdel-Wahab, N.M.; Hassan, H.M.; Perveen, S.; Ameen, F.; Alturki, E.; Abdelmohsen, U.R. Recent updates on the bioactive compounds of the marine-derived genus *Aspergillus*. *RSC Adv.* **2021**, *11*, 17116–17150. [CrossRef]

7. Kruger, G.J.; Steyn, P.S.; Vleggaar, R.; Rabie, C.J. X-ray crystal structure of astelotoxin, a novel mycotoxin from *Aspergillus stellatus* Curzi. *J. Chem. Soc. Chem. Comm.* **1979**, *10*, 441–442. [CrossRef]

8. Kamal, A.; Husain, S.A.; Noorani, R.; Murtaza, N.; Qureshi, I.H.; Quershi, A.A. Studies in the biochemistry of microorganisms. XI. Isolation of tajixanthone, shamixanthone, ajamxanthone, shahenxanthone, najamxanthone, radixanthone and mannitol from mycelium of *Aspergillus stellatus,* Cruzi. *J. Sci. Indus. Res.* **1970**, *13*, 251–255.

9. Prompanya, C.; Dethoup, T.; Bessa, L.J.; Pinto, M.M.M.; Gales, L.; Costa, P.M.; Silva, A.M.S.; Kijjoa, A. New isocoumarin derivatives and meroterpenoids from the marine sponge-associated fungus *Aspergillus similanensis* sp. nov. KUFA 0013. *Mar. Drugs* **2014**, *12*, 5160–5173. [CrossRef]

10. Manojlović, I.; Bogdanović-Dusanović, G.; Gritsanapan, W.; Manojlović, N. Isolation and identification of anthraquinones of *Caloplaca cerina* and *Cassia tora*. *Chem. Pap.* **2006**, *60*, 466–468. [CrossRef]

11. Hawas, U.W.; El-Beih, A.A.; El-Halawany, A.M. Bioactive anthraquinones from endophytic fungus *Aspergillus versicolor* isolated from red sea algae. *Arch. Pharm. Res.* **2012**, *35*, 1749–1756. [CrossRef] [PubMed]

12. Noinart, J.; Buttachon, S.; Dethoup, T.; Gales, L.; Pereira, J.A.; Urbatzka, R.; Freitas, S.; Lee, M.; Silva, A.M.S.; Pinto, M.M.M.; et al. A new ergosterol analog, a new bis-anthraquinone and anti-obesity activity of anthraquinones from the marine sponge-associated fungus *Talaromyces stipitatus* KUFA 0207. *Mar. Drugs* **2017**, *15*, 139. [CrossRef] [PubMed]

13. Wen, H.; Chen, C.; Sun, W.; Zang, Y.; Li, Q.; Wang, W.; Zeng, F.; Liu, J.; Zhou, Y.; Zhou, Q.; et al. Phenolic *C*-glycosides and aglycones from marine-derived *Aspergillus* sp. and their anti-inflammatory activities. *J. Nat. Prod.* **2019**, *82*, 1098–1106. [CrossRef]

14. Pornpakakul, S.; Liangsakul, J.; Ngamrojanavanich, N.; Roengsumran, S.; Sihanonth, P.; Piapukiew, J.; Sangvichien, E.; Puthong, S.; Amorn Petsom, A. Cytotoxic activity of four xanthones from *Emericella variecolor,* an endophytic fungus isolated from *Croton oblongifolius*. *Arch. Pharm. Res.* **2006**, *29*, 140–144. [CrossRef]

15. Figueroa, M.; González, M.C.; Rodríguez-Sotres, R.; Sosa-Peinado, A.; González-Andrade, M.; Cerda-Gárcıa-Rojas, C.M.; Mata, R. Calmodulin inhibitors from the fungus *Emericella* sp. *Bioorg. Med. Chem.* **2009**, *17*, 2167–2174. [CrossRef] [PubMed]

16. González, A.M.; Rivera, C.J.; Sosa, P.A.; Figueroa, M.; Rodríguez-Sotres, R.; Mata, R. Development of the fluorescent biosensor h Calmodulin (h CaM) L39C-monobromobimane (mBBr)/V91C-mBBr, a novel tool for discovering new calmodulin inhibitors and detecting calcium. *J. Med. Chem.* **2011**, *54*, 3875–3884. [CrossRef] [PubMed]

17. Takenaka, Y.; Hamada, N.; Tanahashi, T. Aromatic compound from cultured lichen mycobionts of the three *Graphis* species. *Heterocycles* **2011**, *83*, 2157–2164.

18. Damodaran, V.; Ryan, J.L.; Keyzers, R.A. Cyclic 3-alkyl pyridinium alkaloid monomers from a New Zealand *Haliclona* sp. marine sponge. *J. Nat. Prod.* **2013**, *76*, 1997–2001. [CrossRef]

19. Schmidt, G.; Timm, C.; Köck, M.; Haliclocyclin, C. A new monomeric 3-alkyl pyridinium alkaloid from the arctic marine sponge *Haliclona viscosa*. *Z. Naturforsch.* **2011**, *66b*, 745–748. [CrossRef]

20. Maarisit, W.; Abdjul, D.B.; Yamazaki, H.; Kato, H.; Rotinsulu, H.; Wewengkang, D.S.; Sumilat, D.A.; Kapojos, M.M.; Ukai, K.; Namikoshi, M. Anti-mycobacterial alkaloids, cyclic 3-alkyl pyridinium dimers, from the Indonesian marine sponge *Haliclona* sp. *Bioorg. Med. Chem. Lett.* **2017**, *27*, 3503–3506. [CrossRef]

21. Markam, K.R.; Mues, R.; Stoll, M.; Zinsmeister, H.D. NMR spectra of flavone di-C-glycosides from *Apometzgeria pubescens* and the detection of rotational isomerism in 8-C-hexosylflavone. *Z. Naturforsch.* **1987**, *42c*, 1039–1042. [CrossRef]

22. Chexal, K.K.; Fouweather, C.; Holker, J.S.E.; Simpson, T.J.; Young, K. The biosynthesis of fungal metabolites. Part III. Structure of shamixanthone and tajixanthone, metabolites of *Aspergillus variecolor*. *J. Chem. Soc. Perkin Trans.* **1974**, *1*, 1584–1593. [CrossRef]

23. Chexal, K.K.; Holker, J.S.E.; Simpson, T.J. The biosynthesis of fungal metabolites. Part VI. Structure and biosynthesis of some minor metabolites from variant strains of *Aspergillus variecolor*. *J. Chem. Soc. Perkin Trans.* **1975**, *1*, 549–554. [CrossRef]

24. Luís, A.; Cruz, C.; Duarte, A.P.; Domingues, F. An alkenylresorcinol derivative from *Hakea sericea* fruits and their antimicrobial activity. *Nat. Prod. Com.* **2013**, *8*, 1459–1462. [CrossRef]

25. Hafez Ghoran, S.; Fatemeh Taktaz, F.; Ayatollahi, S.A.; Kijjoa, A. Anthraquinones and their analogues from marine-derived fungi: Chemistry and biological activities. *Mar. Drugs* **2022**, *20*, 474. [CrossRef] [PubMed]

26. de Sá, J.D.M.; Pereira, J.A.; Dethoup, T.; Cidade, H.; Sousa, M.E.; Rodrigues, I.C.; Costa, P.M.; Mistry, S.; Silva, A.M.S.; Kijjoa, A. Anthraquinones, diphenyl ethers, and their derivatives from the culture of the marine sponge-associated fungus *Neosartorya spinosa* KUFA 1047. *Mar. Drugs* **2021**, *19*, 457. [CrossRef]

27. Murray, M.G.; Thompson, W.F. Rapid isolation of high molecular weight plant DNA. *Nucleic Acids Res.* **1980**, *8*, 4321–4326. [CrossRef]

28. White, T.J.; Bruns, T.; Lee, S.; Taylor, J. Amplification and direct sequencing of fungal ribosomal RNA genes for phylogenetics. In *PCR Protocols: A Guide to Methods and Applications*; Innis, M.A., Gelfand, D.H., Sninsky, J.J., White, T.J., Eds.; Academic Press: New York, NY, USA, 1990; pp. 315–322.

29. Sanger, F.; Nicklen, S.; Coulson, A.R. DNA sequencing with chain-terminating inhibitors. *Proc. Natl. Acad. Sci. USA* **1977**, *72*, 5463–5467. [CrossRef]

30. Sheldrick, G.M. A short history of SHELX. *Acta Crystallogr. Sect. A* **2008**, *A64*, 112–122. [CrossRef]

31. Flack, H.D. On enantiomorph-polarity estimation. *Acta Crystallogr. Sect. A* **1983**, *39*, 876–881. [CrossRef]

32. Stephens, P.J.; Harada, N. ECD Cotton effect approximated by the Gaussian curve and other methods. *Chirality* **2010**, *22*, 229–233. [CrossRef] [PubMed]

33. Simões, R.R.; Aires-de-Sousa, M.; Conceição, T.; Antunes, F.; da Costa, P.M.; de Lencastre, H. High prevalence of EMRSA-15 in Portuguese public buses: A worrisome finding. *PLoS ONE* **2011**, *6*, e0017630. [CrossRef] [PubMed]

34. Bessa, L.J.; Barbosa-Vasconcelos, A.; Mendes, Â.; Vaz-Pires, P.; Da Costa, P.M. High prevalence of multidrug-resistant *Escherichia coli* and *Enterococcus* spp. in river water, upstream and downstream of a wastewater treatment plant. *J. Water Health* **2014**, *12*, 426–435. [CrossRef]

35. CLSI. *Performance Standards for Antimicrobial Susceptibility Testing*, 28th ed.; CLSI supplement M100; Clinical and Laboratory Standards Institute: Wayne, PA, USA, 2018.

36. CLSI. *Performance Standards for Antimicrobial Disk Susceptibility Tests; Approved Standard*, 11th ed.; CLSI Document M02-A11; Clinical and Laboratory Standards Institute: Wayne, PA, USA, 2012.

37. CLSI. *Methods for Dilution Antimicrobial Susceptibility Tests for Bacteria that Grow Aerobically*, 11th ed.; CLSI Standard M07; Clinical and Laboratory Standards Institute: Wayne, PA, USA, 2018.

38. CLSI. *Methods for Determining Bactericidal Activity of Antimicrobial Agents; Approved Guideline*; CLSI Document M26-A; Clinical and Laboratory Standards Institute: Wayne, PA, USA, 1999.

39. Kumla, D.; Dethoup, T.; Gales, L.; Pereira, J.A.; Freitas-Silva, J.; Costa, P.M.; Silva, A.M.S.; Pinto, M.M.M.; Kijjoa, A. Erubescensoic acid, a new polyketide and a xanthonopyrone SPF-3059-26 from the culture of the marine sponge-associated fungus *Penicillium erubescens* KUFA 0220 and antibacterial activity evaluation of some of its constituents. *Molecules* **2019**, *24*, 208. [CrossRef] [PubMed]

40. Gomes, N.M.; Bessa, L.J.; Buttachon, S.; Costa, P.M.; Buaruang, J.; Dethoup, T.; Silva, A.M.S.; Kijjoa, A. Antibacterial and antibiofilm activities of tryptoquivalines and meroditerpenes isolated from the marine-derived fungi *Neosartorya paulistensis*, *N. laciniosa*, *N. tsunodae*, and the soil *fungi N. fischeri* and *N. siamensis*. *Mar. Drugs* **2014**, *12*, 822–839. [CrossRef]

41. Odds, F.C. Synergy, antagonism, and what the chequer board puts between them. *J. Antimicrob. Chemother.* **2003**, *52*, 1. [CrossRef]

42. Stepanović, S.; Vuković, D.; Hola, V.; Di Bonaventura, G.; Djuki'c, S.; Cirković, I.; Ruzicka, F. Quantification of biofilm in microtiter plates: Overview of testing conditions and practical recommendations for assessment of biofilm production by staphylococci. *Apmis* **2007**, *115*, 891–899. [CrossRef] [PubMed]